# Positronium diffusion in porous methylsilsesquioxane thin films*

Dong Xi-Jie(董锡杰)[a)b)], Hu Yi-Fan(胡一帆)[b)†], and Wu Yu-Ying(吴玉莹)[a)b)]

[a)] *Wuhan High Magnetic Field Center, Huazhong University of Science and Technology, Wuhan* 430074, *China*
[b)] *School of Physics, Huazhong University of Science and Technology, Wuhan* 430074, *China*

(Received 7 October 2008; revised manuscript received 13 August 2009)

Depth profiled positronium (Ps) annihilation lifetime spectroscopy (PALS) is an extremely useful probe of the pore characteristics in nanoporous low-dielectric (low-$k$) constant thin films. PALS has also been considered as a potential probe to investigate diffusion barrier integrity and the structural changes of porous low-$k$ films during their integration with Cu. Hence, it is essential to understand the diffusion behaviour of positronium/Cu atoms in the films. In this work, based on the fact that porous materials possess characteristics of statistical self-similarity, a fractal model, the Menger sponge model, has been applied to simulate the structure of a promising dielectric, porous methylsilsesquioxane (MSQ) films. The diffusion behaviour of Ps out of the fractal model and into the surrounding vacuum is studied by means of the diffusion equation and traditional advective–diffusive theory. Predictive results from our model show good agreement with measurement data.

**Keywords:** positronium, porous methylsisesquioxane thin films, low-$k$, Menger sponge model
**PACC:** 3610, 6140G, 7755, 0555

## 1. Introduction

With increasing requirements for electrical performance of on-chip wiring, resistance–capacitance (RC) delay, electric power consumption and cross talk become dominant factors restricting the development of ultra-large-scale integrated circuits. Low-$k$ materials are found to be promising materials for meeting these requirements. One of the promising materials, porous methylsilsesquioxane (MSQ) film, has many merits such as a low-$k$ low to 2.3,[1] attractive adhesion to metals[2] and high thermal stability.[3] The dielectric properties and mechanical properties of MSQ dielectrics indicate that MSQ is a promising dielectric However, the structures of the porous MSQ thin films are not well understood yet.

Recently, advanced non-destructive method, beam-based positron annihilation lifetime spectroscopy (PALS), has been developed to characterize the pore information and demonstrated to be a powerful tool in determining interconnected or closed porous structure in low-$k$ films.[4] Since the mechanism responsible for positron emission from porous materials is not yet fully understood, modelling positronium (Ps) diffusion in porous films can help to probe the pore sizes and differentiate open from closed porosity. Moreover, PALS may be used to investigate diffusion barrier integrity and the structural changes of porous low-$k$ films during their integration with Cu. Hence, it is essential to understand the diffusion behaviour of positronium/Cu atoms in the films. Through investigations with a slow positron beam, Knight *et al.*[5] found evidence of Ps formation within the porous layer. Positrons injected in a solid reach thermal energies, then they are efficiently trapped in open structure after a diffusion path and there they annihilate with an electron.[6] In porous media, positrons are favorably trapped in the pores and capture electrons, then form Ps. Positrons are very sensitive to free volume sizes present in a material. Based on the fundamental volume sizes present in materials which can be obtained by the measured positron lifetime, PALS can be used to measure both open voids and closed pores.

The surface of films has been considered to play a dominant role in determining some properties of materials. Using the positrons to demonstrate the investigation of surface is an earlier work.[7] The surface area in porous material is extremely large,[8] thus we introduce a fractal model to find the ratio of the actual surface area to the cross-sectional area ($\eta$) and describe the rough surface construction of porous material in the next part of the article.

*Project supported by the National Natural Science Foundation of China (Grant No. 60476011).
†Corresponding author. E-mail: yifanhu2007@yahoo.com.cn
© 2010 Chinese Physical Society and IOP Publishing Ltd

In this paper, we try to study the positronium diffusion in porous MSQ in theory. To study dielectric properties and mechanical properties, we consider that establishing a theoretical model for pore structure is crucial. Molecular dynamics simulations of porous materials showed that the structure of this type of nanoporous low-$k$ dielectrics[9,10] exhibits fractal-like behaviour, which might be their characteristic. Thus we focus on establishing a model to describe Ps diffusion in porous MSQ films.

## 2. The ratio of the surface area to the cross-sectional area

In porous dielectrics, there are numerous irregular pores with different sizes. The pore microstructures, both the pore size and the pore-interfaces, of such porous media exhibit fractal characteristics.[11−20] The porous dielectrics, following Eq. (1), are considered as fractal porous dielectrics,

$$M(L) \sim L^{D_f}, \tag{1}$$

where $D_f$ is the fractal dimension, $L$ is the length scale, $M(L)$ could be the length of a line or the area of a surface or the volume or the mass of an object.

Porous films contain pores within a large radius interval, so it can be associated with the Menger sponge fractal model[21] (shown in Fig. 1). The volume fractal dimension of an exactly fractal Menger sponge can be expressed as

$$D_{\mathrm{V}} = \frac{\ln(L^3 - 7C^3)}{\ln L}, \tag{2}$$

where $C$ is the cut-out size and $D_{\mathrm{V}}$ is the fractal dimension of pores in three dimensions. It is a unique property of the Menger sponge that its surface fractal dimension ($D_{\mathrm{S}}$) and volume fractal dimension ($D_{\mathrm{V}}$) are equal,[21] namely,

$$D_{\mathrm{S}} = D_{\mathrm{V}} = \frac{\ln(L^3 - 7C^3)}{\ln L}. \tag{3}$$

The volume porosity of the Menger sponge, $\phi_{\mathrm{V}}$, is given by

$$\phi_{\mathrm{V}} = \frac{V_0 - V_n}{V_0} = 1 - \left(\frac{L^3 - 7C^3}{L^3}\right)^{n+1}, \tag{4}$$

where $V_0$ and $V_n$ are the initial volume and the volume of the framework at $n$ (0, 1, 2, ...) stage.

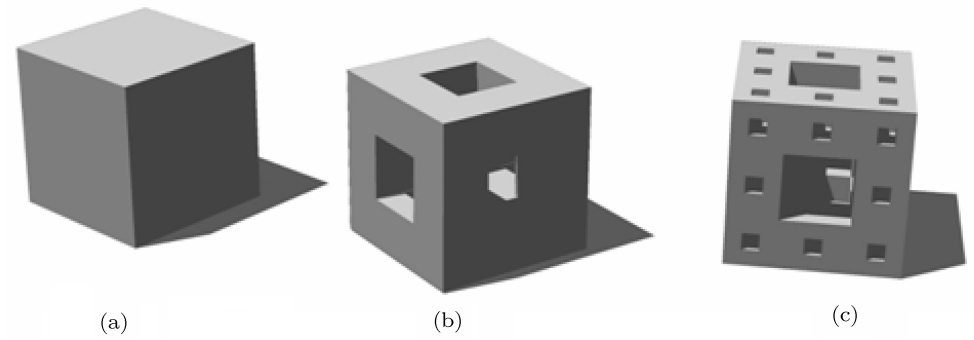



**Fig. 1.** The transformation to the Menger sponges of stages (b) $n = 1$ and (c) $n = 2$ from a cube (a).

At the surface, actual area could be estimated as the cross-sectional area and the area perpendicular to the cross section of the pore surface. The two-dimensional projection of the Menger sponge is the Sierpinski carpet (shown in Fig. 2). It could be obtained that the ratio of the surface area to the cross-sectional area is

$$\eta = \frac{S + \Delta S}{S}, \tag{5}$$

where $S$ is the cross-sectional area, $\eta$ is the ratio of the actual surface area to the cross-sectional area, and $\Delta S$ is the area of the four sides of the pore surface which are perpendicular to the surface.

The cut-out area of the Sierpinski carpet can also be obtained as in Ref. [22]

$$A'_{\mathrm{tn}} = L^2\left[1 - \left(\frac{L^2 - C^2}{L^2}\right)^{n+1}\right]. \tag{6}$$

Based on the structure of the Menger sponge, $\Delta S$ can be expressed as

$$\Delta S = 4A'_{\rm tn}. \tag{7}$$

According to Eqs. (3), (4), and (6), we can obtain the relation between porosity and actual surface area

$$\eta = 4[1-(1-\phi_{\rm V})^{\frac{\ln((L^2-C^2)/L^2)}{(D_{\rm S}-3)\ln L}}]+1. \tag{8}$$

The surface fractal dimension of phenylsilsesquioxane is 2.57[23] under the circumstances we discussed. Because MSQ synthesized under the same condition has a similar structure to phenylsilsesquioxane, the surface fractal dimension of MSQ has the same value. Thus we use the Menger sponge with $L = 11$ and $C = 5$ (fractal dimension is 2.55) to simulate the structure of porous MSQ films.

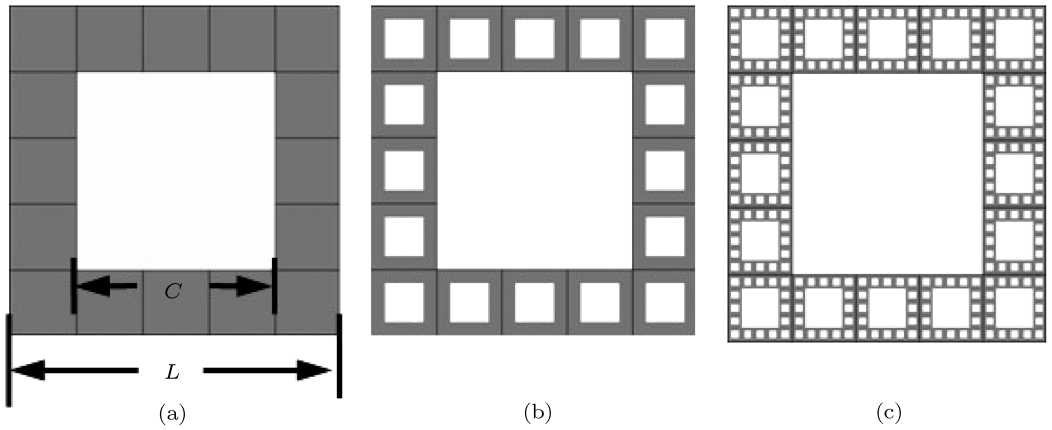



**Fig. 2.** The Sierpinski carpets of fractal dimension $D = 1.723$ at stages (a) $n = 0$, (b) $n = 1$, and (c) $n = 2$.

## 3. Diffusion model and simulation method

In this section, we try to obtain the analytical expression of Ps intensity measured in vacuum. The ratio of the surface area to the cross-sectional area, $\eta$ (described in the last section), which plays an important role in the formation of Ps, will be a necessary parameter to calculate the intensity of Ps annihilated in vacuum. The intensity of Ps will be described by several parts in this section.

### 3.1. Porosity and porogen loading

In typical low-$k$ film pore generation schemes, an amount of pore generator (porogen) is mixed with a low-$k$ matrix precursor in solution and then spin cast to form a nanocomposite film. After high temperature treatment, the porogen is burnt and leaves pores behind. The exact relation of porosity and porogen loading is not yet known.

Yang *et al.*[24] have reported the dielectric constant in different porogen loading data. We use the Clausius–Mossotti effective medium model to find the relation between porosity and porogen loading. The simplest expression of the Clausius–Mossotti effective medium model applied to two-phase materials is given by

$$\frac{\varepsilon_{\rm r}-1}{\varepsilon_{\rm r}+2} = (1-\phi_{\rm V})\cdot\frac{(\varepsilon_2-1)}{(\varepsilon_2+2)}, \tag{9}$$

where $\varepsilon_2$ is the relative dielectric constant of the dense MSQ, and $\varepsilon_{\rm r}$ is a rough estimate of the dielectric constant of the porous media.[25] These values are related to the porosity $\phi_{\rm V}$ of the porous media. With about 45% of the total porosity, the dielectric constant for MSQ-based films is about 2.0.[26] According to Eq. (9), the calculated dielectric constant of dense MSQ, $\varepsilon_2$ is about 3.5. By using Eq. (9), we can fit the experimental data, and the relationship between porosity and porogen loading, $x$, can be deduced as

$$\phi_{\rm V} = 0.1375 + x. \tag{10}$$

From refractive index measurements, Petkov *et al.* considered that the factor of porosity and porogen loading is $0.77 \pm 0.01$,[27] namely,

$$\phi_{\rm V} = 0.77x. \tag{11}$$

Figure 3 shows the comparison of the experimental data and the predictions. It is obvious that the dielectric constants predicted by Eq. (10) are in better agreement with the experimental data than those by Eq. (11). According to Eq. (10), we can obtain that the porosity is 14.75% when the porogen loading is 1%, which is identical to the film with 1% of porogen, which already contains 14 vol.%–16 vol.% micro-pores.[4]

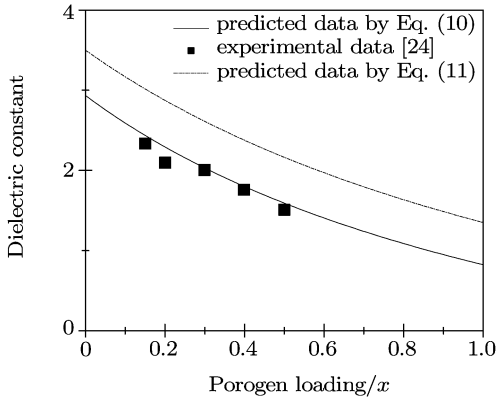



**Fig. 3.** A comparison of the dielectric constant predicted by Eq. (11), with existing experimental data[24] and that predicted by Eq. (10).

## 3.2. Ps branching ratio for MSQ surface

Researchers have found that at glancing incidence, electron captured by surface-reflected positrons formed a variable 'fast' (10–100 eV) energy Ps beam with intensity up to 3%–5% probability on the surfaces of Al and Cu.[28] In a thin epoxy resin film on a Si substrate, the Ps intensity increased slightly and then decreased continuously from about 27% to a very small value of less than 2% as a function of the incident positron energy (1–4 keV) in 45 nm thick films.[29] In this work, the incident positron energy discussed is between 1 and 8 keV, we neglect the effect of incident positron energy on 'fast' Ps and estimate the average. Thus the 'fast' Ps intensity can be considered to be less than 2%[29] and thus the 'fast' Ps intensity in porous MSQ films is estimated to be 1.6% according to Ref. [2]. We label the intensity of 'fast' Ps as $f_{\rm Ps0}$, i.e.,

$$f_{\rm Ps0} = 0.016. \tag{12}$$

The three-dimensional diffusion equation of Ps in films is given by

$$\frac{\partial n(r,t)}{\partial t} = D_+ \nabla^2 n(r,t) - \lambda n(r,t), \tag{13}$$

where $D_+$ is the positron diffusion coefficient in the film, $n(r,t)$ is the positron density as a function of both time and position, and $(\lambda^{-1} = \tau)$ is the effective lifetime of the positron in a freely diffusing state $(4.59 \times 10^{-9}\ {\rm s}^{-1})$.[30]

Without internal reflection at the surface and by solving in the trivial case of an initial profile, a $\delta$-function $(\psi(z,0) = \delta(z-a))$, the general solution for the positron wavefunction density is the integration over the solution in Eq. (13) and is expressed by

$$\psi(a,z,t) = \left\{ \sqrt{\pi} \frac{\exp\left[-\dfrac{(a-z)^2}{4D_+t}\right] - \exp\left[-\dfrac{(a+z)^2}{4D_+t}\right]}{2\sqrt{D_+t}} \right\} \exp[-\lambda t]. \tag{14}$$

The number of positions which diffuse back to the surface can be given by

$$N(a,z,t) = |J(z,t)| = D_+ \left[\frac{\partial \psi}{\partial z}\right], \tag{15}$$

where $J(z,t)$ means the positron current through the position $z$ at time $t$. The total flux through the plane at the position $z$ is

$$\begin{aligned} N(a,z) &= \int_0^\infty N(a,z,t){\rm d}t \\ &= \frac{1}{2}(\exp[-\sqrt{(a-z)^2/D_+\tau}] + \exp[-\sqrt{(a+z)^2/D_+\tau}]) \\ &= \frac{1}{2}(\exp[-(a-z)/L_+] + \exp[-(a+z)/L_+]), \end{aligned} \tag{16}$$

where $L_+$ is the diffusion length in angstrom given by

$$L_+ = \sqrt{D_+\tau} = (A/A')E_0^n \tag{17}$$

with $n$ a constant. The constant $A$ can be found empirically to be $A \sim (400/\rho)$, Å/keV$^n$ where $\rho$ is the target density in g/cm$^3$, $E$ is in keV, and $A'$ depends on the profile.[31] Calculated by a combination of EP and SAWS data, the typical skeleton density of the MSQ films is close to 1.4 g/cm$^3$,[4] and we label the dense density as $\rho_0$. The density of porous film and the constant $A$ can be expressed as

$$\rho = \rho_0(1-\phi), \tag{18}$$

$$A{\sim}(400/\rho_0)/(1-\phi). \tag{19}$$

If $L_{+0}$ denotes the mean diffusion length of the dense MSQ film, due to Eqs. (18) and (19), the mean diffusion length of the porous MSQ is given by

$$L_+ = \frac{L_{+0}}{1-\phi} = \frac{\sqrt{D_{+0}\tau}}{1-\phi}, \tag{20}$$

where $D_{+0}$ is 0.1 cm$^2$/s.[32]

After thermalization in the polymer, a positron reaching to the pore surface has a chance to form Ps. The probability of Ps formation is related to the branching ratio for Ps and the surface roughness. The larger the roughness of the surface is, the bigger the probability of Ps formation is. So we introduce the ratio of the effective surface area to the cross-sectional area to estimate the intensity of Ps at the surface. The probability $f_{\rm Ps1}(0)$ of a positron reaching the near surface and then forming positronium (Ps) is expressed as

$$f_{\rm Ps1}(0) = f_0\eta \int_0^l p(a,E)N(a,z)\mathrm{d}a\Big|_{z=0}, \tag{21}$$

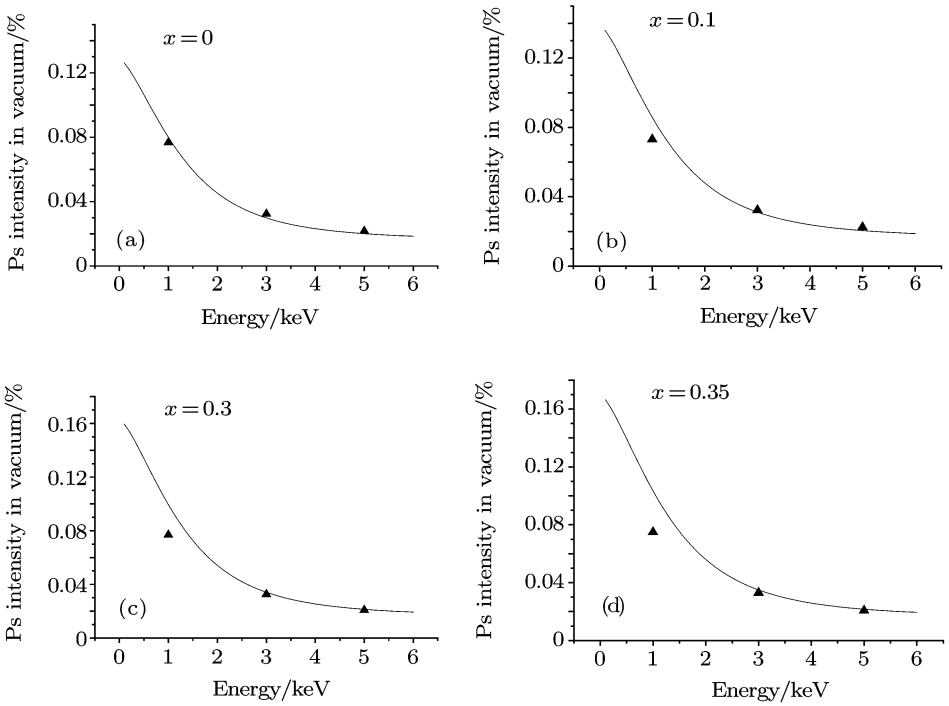
where $\eta$ is the ratio of the surface area to the cross-sectional area described in Section 2, $l$ is the thickness of porous MSQ films, $f_0$ is the branching ratio for Ps, and $p(a,E)$ is the implantation profile of the positrons after thermalization in the polymer. The implantation profile is expressed as

$$p(a,E) = m\frac{a^{m-1}}{z_0^m}\exp\left[-\left(\frac{a}{z_0}\right)^m\right], \tag{22}$$

where $z_0 = AE^n/\Gamma(1/m+1)$, $m$ is a constant.[31] For MSQ films, $n$ is 1.44[4] and $m$ is set to 2.

In the case that pores are closed, Ps forming in the porous films cannot reach the surface. Thus, the measured intensity includes 'fast' Ps ($f_{\rm Ps0}$) and Ps forming on the near surface ($f_{\rm Ps1}$). Based on Eqs. (12) and (21), the best fit of experimental data[33] shown in Fig. 3 gives a value of $f_0 = 0.1$ in MSQ films.

Figure 4 shows that the theoretical intensity shows a good agreement with the experimental data at $x = 0$ and $x = 0.1$, when $f_0 = 0.1$.



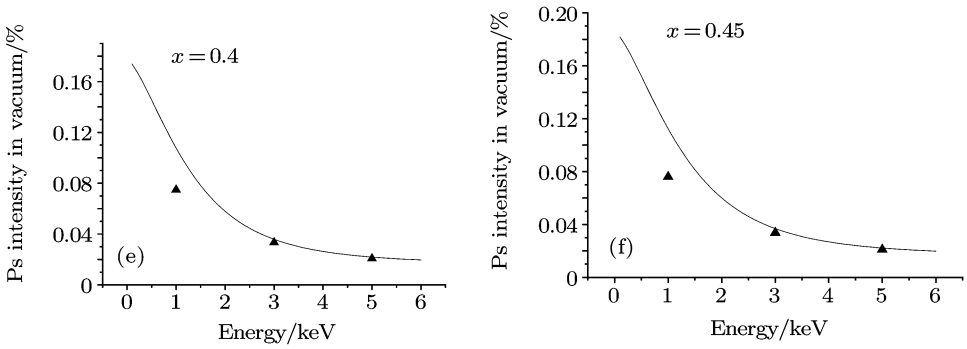



**Fig. 4.** According to Eqs. (12) and (21) and $f_0 = 0.1$, a comparison of the present model predictions with the experimental data in Ref. [33] is shown for different porogen loading, $x$, before pores are interconnected.

### 3.3. Ps diffusion in porous dielectric

For porous films, there is a critical porogen loading, the connectivity threshold ($x_{\text{threshold}}$), above which pores become interconnected with the surface. Above the percolation threshold, atomic Ps gas can diffuse through a long distance. Ps gas diffusion in porous media is an important factor in flow.

Based on the advective–diffusive model, the mass flux for one gas component, neglecting gravity and the Klinkenberg factor, can be obtained as[34]

$$F = -\frac{k_0}{\mu_{\text{Ps}}}\rho_{\text{Ps}}\nabla P_{\text{Ps}}, \tag{23}$$

where $F$ is the mass flux for Ps gas (kg/(m$^2$·s)), $k_0$ is intrinsic permeability (m$^2$), $\mu_{\text{Ps}}$ is viscosity (kg/(m·s)), $\rho_{\text{Ps}}$ is density of the Ps gas (kg/m$^3$), and $P_{\text{Ps}}$ is the pressure (Pa). We denote the ratio of intrinsic permeability to viscosity as

$$\gamma = \frac{k_0}{\mu_{\text{Ps}}}. \tag{24}$$

According to the ideal-gas equation of state and the relation between mass density and number density, Eq. (23) can be rewritten as

$$F = -(\gamma\kappa T m_{\text{Ps}})n_{\text{Ps}}\nabla n_{\text{Ps}}, \tag{25}$$

where $\kappa$ is Boltzmann's constant, $m_{\text{Ps}}$ is the mass of Ps, and $T$ is the temperature (K).

When positrons diffuse around the pores, positrons can capture electrons around the pore surface and form Ps. Positron and Ps diffusion processes in a mesoporous sample determine a 'sensitivity volume' around a pore, which can probe the pore structure.[27] Figure 5 shows the ideal porous structure, where $d$ is the average pore distance indicating the average centre-to-centre distance between two adjacent pores.

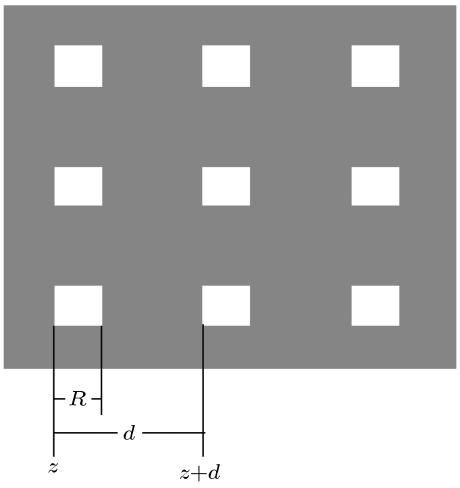



**Fig. 5.** Illustration of pores in films.

With the assumption that pores are rectangular, a cell including one pore is shown in Fig. 6. The average volume porosity and the average area porosity are equal,[35] the porosity relabelled as $\phi$ can be expressed as

$$\phi = \frac{R^2}{d^2}. \tag{26}$$

The approximate average pore distance can be obtained as

$$d = \frac{R}{\sqrt{\phi}}. \tag{27}$$

When positrons ($N_0$) are implanted into the film, the positrons which can reach position $z$ could diffuse freely in the pore volume $SR\phi$, where $S$ is the cross-sectional area of the films implanted with positrons. The number density of Ps through position $z$ at time

$t$, $n_{\rm Ps}$ can be given by

$$n_{\rm Ps} = \frac{N_0 f_{\rm Ps}(z,t)}{SR\phi} = \frac{n_0 l f_0}{R}\left[\int_z^{z+d} p(a)N(a,z,t)\mathrm{d}a\right], \quad (28)$$

where ${}_0n = N_0/Sl$ is the number density of incident positrons.

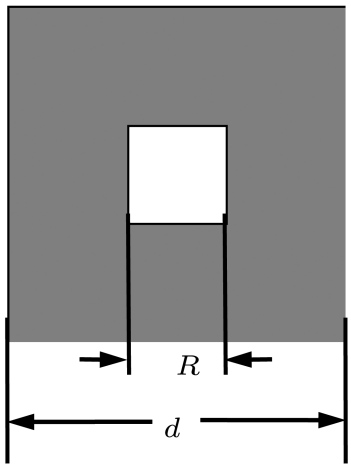



**Fig. 6.** Illustration of the average pore distance by a cell model including one pore.

The total mass flux for Ps which can reach the surface by diffusing out through interconnected pores is given by

$$F(0) = \int_0^{\infty} F(z,t)\mathrm{d}t\Big|_{z=0}. \quad (29)$$

At the film surface, the intensity of Ps ($f_{\rm Ps2}$) diffusing out of interconnected pores is

$$f_{\rm Ps2} = \frac{F(0)\cdot\phi S/m_{\rm Ps}}{N_0} = \frac{\gamma\kappa T(n_0 l)f_0^2}{R^2}\phi p(d) \times \int_0^{\infty}\left[\int_0^{d} p(a)N(a,0,t)\mathrm{d}a\right]N(d,0,t)\mathrm{d}t. \quad (30)$$

The intensity of Ps measured at the surface includes the 'fast' Ps intensity, the intensity of Ps forming at the surface after thermalization, and the intensity of the Ps diffusing out of the interconnected pores. So the measured intensity $I_{\rm Ps}$ can be expressed by

$$I_{\rm Ps} = f_{\rm Ps0} + f_{\rm Ps1} + \theta(x - x_{\rm threshold})f_{\rm Ps2}, \quad (31)$$

where the step function $\theta(x - x_{\rm threshold})$ sets the Ps intensity diffusing out of the interconnected pores to zero when porosity is below the percolation threshold of the material (i.e., no interconnected pores). Equation (31) can be used to predict the Ps intensity measured in vacuum.

Rosowsky[36] introduced an analytical method to compute the site percolation threshold, and found that the approximate value of percolation threshold is larger than or equal to the real value. The critical porosity of square pores is found to be 0.59.[36] According to Eq. (10), the percolation threshold of porogen loading can be obtained, and the value is about 0.454.

While the pores are interconnected after the porogen loading reaches percolation threshold, interconnected porosity, $\phi$, is equivalent to $(x - x_{\rm threshold})$. Hu *et al.* measured the Ps intensity in vacuum versus porogen weight fraction for different incident energies.[33] Based on Eqs. (12), (21), (30), and the experimental data,[33] the fitting curves are plotted in Fig. 7, compared with the experimental data.

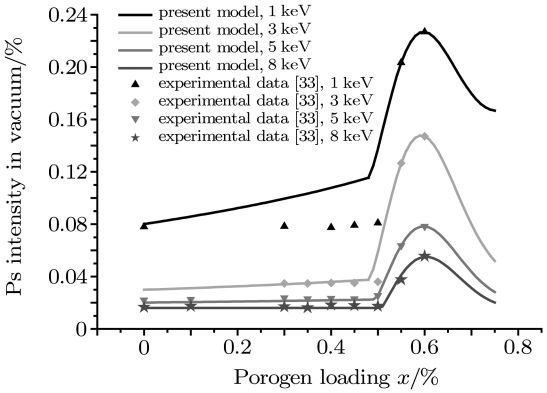



**Fig. 7.** Variation of positron incident energy versus porogen loading weight fraction, a comparison of Ps intensities predicted by the present model with the existing experimental data in the vacuum.

Figure 7 shows the model predictions, which also depicts the effect of the porogen loading and energy on the Ps intensity measured in vacuum. The predictions with 3 keV, 5 keV and 8 keV are in good agreement with existing experimental data but the prediction with 1 keV has a gap. The main reason is that we have ignored the 'fast' Ps change with incident energy. Based on the implantation profile of the positrons, the number of 1 keV positrons implanted into films is the highest of all. Thus the number of surface-reflected positrons is much more than for other cases, that is the 'fast' Ps is much more. In our model, we estimate that the 'fast' Ps beam is 0.016 which is the main reason for the gap produced for 1 keV porositrons. The number of implantation positrons with energies 3 keV, 5 keV and 8 keV is of little difference.

It can be seen that the Ps intensity measured in vacuum increases as the porogen loading increases before the porogen loading reaches a threshold, and then decreases after the peak. The larger the porosity is, the thinner the skeleton films. Accroding to the implantation profile of the positrons after thermalization in the polymer (Eq. (22)), the number of positrons diffusing out of the films increases with the increase of porosity. If the porosity goes on increasing, the intensity would reach the peak value. As the porosity increases further, more positrons enter the substrate through films, and cannot form Ps, which would lead to the decrease of the intensity of Ps annihilated in vacuum. The chance of electrons captured by positrons diffusing through interconnected pores increases with the porogen loading fraction, leading to the increase of Ps intensity in vacuum. While electron density of films decreases as porogen loading fraction increases, the Ps intensity will decrease when the porogen loading fraction reaches a threshold. The threshold model prediction is in agreement with the experimental data,[27] especially at positron energy between 3 and 8 keV.

## 4. Conclusion

Ps diffusion in porous films is an interesting question. In terms of fractal theories, a new model using a Menger sponge is established to describe the porous MSQ structure based on the statistically self-similar characteristics of porous media. With the advective–diffusive model, an analytical expression for the diffusion behaviour of Ps in nanoporous low-$k$ dielectrics is deduced as a function of energy and porogen loading. The expression obtained by using the proposed model is well understood and in agreement with experimental data, and the present model is thus applicable for prediction of the diffusion behaviour of Ps in real porous media.

## References


[1] Takata M, Ogushi K, Yuba Y, Akasaka Y, Tomioka K, Soda E and Kobayashi 2008 *Thin Solid Films* **516** 847
[2] Seok S I, Ahn C H, Jin M Y, Lee C J and Kang Y 2004 *Mater. Chem. Phys.* **84** 259
[3] Ahner N, Schulz S E, Blaschta F and Rennau M 2007 *Micro. Eng.* **84** 2606
[4] Baklanov M R and Mogilnikov K P 2002 *Microelectron. Eng.* **64** 335
[5] Knights A P, Kowalski G, Saleh A S, Towner A, Patel M I, Rive-Evans P C , Moore M, Gledhill G A, Nossarzewska-Orlowska E and Brzozowski A 1995 *J. Appl. Phys.* **78** 4411
[6] Macchi C, Mariotto G, Karwasz G P, Zecca A, Bettonte M and Brusa R S 2004 *Mat. Sci. Semicond. Process.* **7** 289
[7] Dannefaer S, Wiebe C and Kerr D 2000 *J. Porous Mater.* **7** 323
[8] Dannefaer S, Kerr D, Craigen D, BretagnonT, Taliercio T and Foucaran A 1996 *J. Appl. Phys.* **79** 9110
[9] Nakano A, Bi L, Kalia R K and Vashishta P 1993 *Phys. Rev. Lett.* **71** 85
[10] Beckers J V L and de Leeuw S W 2001 *Int. J. Inorg. Mater.* **3** 175
[11] Katz A J and Thompson A H 1985 *Phys. Rev. Lett.* **54** 132
[12] Krohn C E and Thompson A E 1986 *Phys. Rev.* B **33** 6366
[13] Thovert J F, Wary F and Adler P M 1990 *J. Appl. Phys.* **68** 3872
[14] Adler P M 1996 *J. Hydrology* **187** 195
[15] Smidt J M and Monro D M 1998 *Fractals* **6** 401
[16] Yu B M, Lee L J and Cao H Q 2001 *Fractals* **9** 155
[17] Yu B M and Li J H 2001 *Fractals* **9** 365
[18] Yu B M and Cheng P 2002 *Int. J. Heat Mass Transfer* **45** 2983
[19] Yu B M, Lee L J and Cao H Q 2002 *Polym. Compos.* **23** 201
[20] Yu B M and Liu W 2004 *AIChE J.* **50** 46
[21] Alderborn G and Nyström C 1996 *Pharmaceutical Powder Compaction Technology* (New York: Marcel Dekker) p140
[22] Feng Y J, Yu B M, Zou M Q and Zhang D M 2004 *J. Phys.* D **37** 3030
[23] Prado L A S De A, Radovanovic E, Pastore H O, Yoshida I V P and Torriani I L 2000 *J. Polym. Sci.* Part A: *Polym. Chem.* **38** 1580
[24] Yang S, Mirau P A, Pai C S, Nalamasu O, Reichmanis E, Pai J C, Obeng Y S, Seputro J, Lin E K, Lee H J, Sun J N and Gidley D W 2002 *Chem. Mater.* **14** 369
[25] Mezza P, Phalippou J and Sempere R 1999 *J. Non-Cryst. Solids* **243** 75
[26] Maex K, Baklanov M R, Shamiryan D, Iacopi F, Brongersma S H and Yanovitskaya Z S 2003 *J. Appl. Phys.* **93** 8793
[27] Petkov M P, Wang C L, Weber M H, Lynn K G and Rodbell K P 2003 *J. Phys. Chem.* B **107** 2725
[28] Gidley D W, Mayer R, Frieze W E and Lynn K G 1987 *Phys. Rev. Lett.* **58** 595
[29] He C, Hamada E, Suzuki T, Kumaki T, Kobayashi H, Kondo K and Ito Y 2004 *Appl. Surf. Sci.* **221** 444
[30] Zou X, Webb D P, Chan Y C, Lam Y W, Hu Y F, Gong M, Beling C D and Fung S 1998 *J. Non-Cryst. Solids* **227–230** 105
[31] Schultz P J and Lynn K G 1988 *Rev. Mod. Phys.* **60** 701
[32] Shantarovich V P and Goldanskii V I 1998 *Hyperfine Interactions* **116** 67
[33] Hu Y F, Sun J N and Gidley D W 2005 *Chin. Phys. Lett.* **22** 1488
[34] Webb S W and Pruess K 2003 *Transport Porous Med.* **51** 327
[35] Kong X Y 1999 *Advanced Mechanics of Fluids in Porous Media* (Hefei: Publishing House of University of Science and Tech nology of China) p19
[36] Rosowsky A 2000 *Europ. Phys. J.* B **15** 77